



NRC Publications Archive Archives des publications du CNRC

Deformation behaviour and strength of frozen sand Parameswaran, V. R.

This publication could be one of several versions: author's original, accepted manuscript or the publisher's version. /
La version de cette publication peut être l'une des suivantes : la version prépublication de l'auteur, la version
acceptée du manuscrit ou la version de l'éditeur.

Publisher's version / Version de l'éditeur:

Canadian Geotechnical Journal, 17, 1, pp. 74-88, 1980-02

NRC Publications Record / Notice d'Archives des publications de CNRC:

<https://nrc-publications.canada.ca/eng/view/object/?id=ad5e858c-c635-48c7-99d7-ddfa9c9199e8>
<https://publications-cnrc.canada.ca/fra/voir/objet/?id=ad5e858c-c635-48c7-99d7-ddfa9c9199e8>

Access and use of this website and the material on it are subject to the Terms and Conditions set forth at

<https://nrc-publications.canada.ca/eng/copyright>

READ THESE TERMS AND CONDITIONS CAREFULLY BEFORE USING THIS WEBSITE.

L'accès à ce site Web et l'utilisation de son contenu sont assujettis aux conditions présentées dans le site

<https://publications-cnrc.canada.ca/fra/droits>

LISEZ CES CONDITIONS ATTENTIVEMENT AVANT D'UTILISER CE SITE WEB.

Questions? Contact the NRC Publications Archive team at

PublicationsArchive-ArchivesPublications@nrc-cnrc.gc.ca. If you wish to email the authors directly, please see the first page of the publication for their contact information.

Vous avez des questions? Nous pouvons vous aider. Pour communiquer directement avec un auteur, consultez la première page de la revue dans laquelle son article a été publié afin de trouver ses coordonnées. Si vous n'arrivez pas à les repérer, communiquez avec nous à PublicationsArchive-ArchivesPublications@nrc-cnrc.gc.ca.



7702

Ser
THL
N21d
no. 883
c. 2



National Research
Council Canada

Conseil national
de recherches Canada

BLDG

**DEFORMATION BEHAVIOUR AND STRENGTH
OF FROZEN SAND
ANALYZED**

by V. R. Parameswaran

Reprinted from
Canadian Geotechnical Journal
Vol. 17, No. 1, February 1980
p. 74-88

DBR Paper No. 883
Division of Building Research

Price \$1.50

OTTAWA

NRCC 17992

This publication is being distributed by the Division of Building Research of the National Research Council of Canada. It should not be reproduced in whole or in part without permission of the original publisher. The Division would be glad to be of assistance in obtaining such permission.

Publications of the Division may be obtained by mailing the appropriate remittance (a Bank, Express, or Post Office Money Order, or a cheque, made payable to the Receiver General of Canada, credit NRC) to the National Research Council of Canada, Ottawa. K1A 0R6. Stamps are not acceptable.

A list of all publications of the Division is available and may be obtained from the Publications Section, Division of Building Research, National Research Council of Canada, Ottawa. K1A 0R6.



Deformation behaviour and strength of frozen sand

V. R. PARAMESWARAN

Geotechnical Section, Division of Building Research, National Research Council of Canada, Ottawa, Ont., Canada K1A 0R6

Received April 25, 1979

Accepted October 24, 1979

Uniaxial unconfined compression tests were carried out on frozen saturated Ottawa sand containing about 20% by weight of water, at temperatures between -2 and -15°C , and at strain rates varying between 10^{-7} and 10^{-2} s^{-1} . The compressive strength and the initial tangent modulus increased with increasing strain rate and with decreasing temperature. At -2°C , values of strength and modulus were considerably lower than those predicted by linear extrapolation of the values observed at lower temperatures, on a log-log scale. This could be due to the presence of unfrozen water in the samples at -2°C .

Des essais de compression simple ont été faits sur du sable d'Ottawa gelé, saturé à une teneur en eau de 20%, sous des températures de -2 à -15°C , et à des vitesses de déformation variant de 10^{-7} à 10^{-2} s^{-1} . La résistance en compression et le module tangent initial augmente avec une augmentation de la vitesse de déformation et une diminution de la température. A -2°C , les valeurs de la résistance et du module sont considérablement plus faibles que celles déduites d'une extrapolation linéaire sur une échelle log-log des résultats obtenus à plus basse température. Ceci peut être dû à la présence d'eau non gelée dans les échantillons à -2°C .

[Traduit par la revue]

Can. Geotech. J., 17, 74-88 (1980)

Introduction

Foundations in permafrost areas are usually designed to ensure preservation of the frozen ground. A pile foundation in frozen ground transfers the superimposed loads by two mechanisms: shear along the pile (adfreezing) and end bearing, the former being the major contributing factor. End bearing will be mobilized only after the adfreeze bond between a pile and the frozen ground is broken. The total bearing capacity of a pile is the sum of the calculated contributions of these two mechanisms. Empirical formulae for such calculations have been proposed by several workers in the Soviet Union (Vyalov and Porkhaev 1976), based on their experience with structures in the north.

A design value for end-bearing capacity of a pile can be obtained from the values of the compressive strength of the soil, determined under confined and unconfined conditions, and from long-term creep tests. Although frozen soil provides excellent bearing for structures, its strength is reduced rapidly with increasing temperature and it loses all strength on thawing. Hence for design of foundations the time- and temperature-dependent strength properties of soils are important considerations.

Mechanical properties of frozen soils have been studied in the Soviet Union from as early as 1920 (Tsytoich 1975), but the published material was generally incomplete as to description of soil and testing procedures. Since 1959, however, several Russian

publications describing detailed test procedures and giving extensive experimental data on the strength and deformation properties of frozen natural soils and clays have been translated by the U.S. Army Cold Regions Research and Engineering Laboratories (CRREL), and the National Research Council of Canada (Tsytoich and Sumgin 1959; Tsytoich *et al.* 1973; Vylov 1965*a,b*; Vyalov and Porkhaev 1976).

More recently, several investigators have studied the deformation behaviour of natural and artificially frozen soils under various conditions of temperature and pressure. The mechanical properties of frozen soils are very dependent on soil characteristics such as frozen and unfrozen water contents, grain-size distribution, mineral content, ice lenses and layering, and externally imposed testing conditions such as strain rate, temperature, stress and strain history, and confining pressure. Owing to the varying nature of soils and conditions of experiment, it is difficult to compare or correlate the data obtained by different authors. However, one can still compare the results obtained for materials of the same type (such as quartz sands) tested under similar conditions of strain rate and temperature.

As part of an experimental program of laboratory model studies of foundations in frozen ground undertaken at the Division of Building Research, National Research Council of Canada, investigations were carried out on the temperature- and strain-rate-

dependence of the strength of artificially frozen sand of uniform grain size and composition. In earlier papers (Parameswaran 1978a,b, 1979) the measurement of adfreeze strength under constant rates of loading and under constant loads were reported. This paper contains the results of the study of deformation behaviour and compressive strength of frozen sand as a function of strain rate and temperature. These results are also compared with the results obtained by several earlier workers for similar materials under comparable test conditions.

Experimental Method

Materials and Sample Preparation

The sand used for preparing the test specimens was of the same grain size and composition as that used in earlier tests (Parameswaran 1978a,b, 1979), namely, Ottawa sand (ASTM Specification C-109, passing

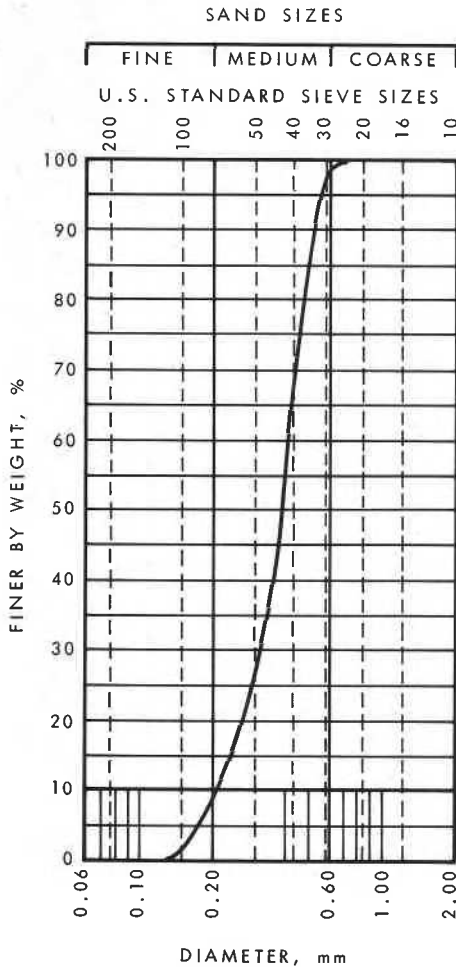


FIG. 1. Grain-size distribution of Ottawa sand.

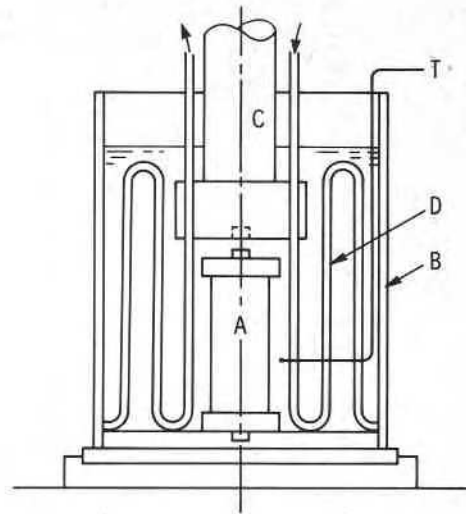


FIG. 2. Schematic diagram of apparatus to measure compressive strength of frozen sand. A = cylindrical sample (50.8 mm in diameter); B = Plexiglas vessel containing kerosene; C = upper compression member from Instron load cell; D = cooling coil; T = thermocouple.

sieve No. 30 and retained on sieve No. 100) mixed with 14% by weight of water. When compacted this mixture had an optimum density of 1700 kg·m⁻³ (106 lb/ft³) as determined by a Proctor test. Figure 1 gives the grain-size analysis of the sand.

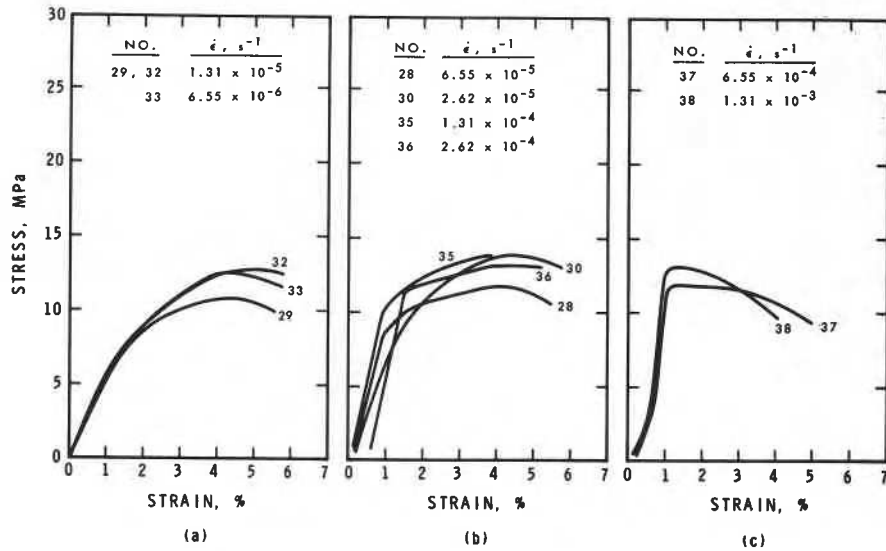
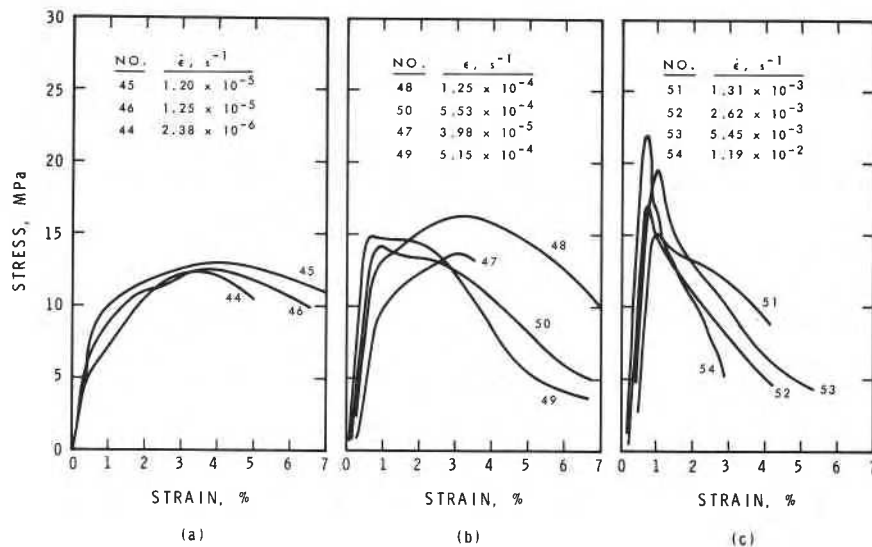
Cylindrical samples of frozen sand having diameter, *D*, of 50.8 mm (2 in.) and length of about 140 mm (5.5 in.) were prepared in a split Plexiglas mould by a method described by Baker (1976). The sand was compacted at optimum moisture content in layers in the mould, which was connected to a vacuum pump to remove the air. After evacuation the sand was saturated with deaerated distilled water prior to freezing.

The specimens were frozen uniaxially in the mould inside an insulated box with the top end exposed to the air inside a cold room at -6°C. The water expelled during freezing was removed from the bottom through a capillary tube containing a heater wire.

After freezing, the ends of a cylindrical sample were trimmed and faced in a lathe inside the cold room, and mounted in stainless-steel end caps using water as a filler material. The finished test specimens had a gauge length, *L*, of about 127 mm (5 in.) between the end caps (so that the *L/D* ratio was greater than 2), and a total moisture content of about 20% by weight of soil grains.

Test Procedure

The cylindrical samples of frozen sand were tested under uniaxial compression in a floor-model Instron

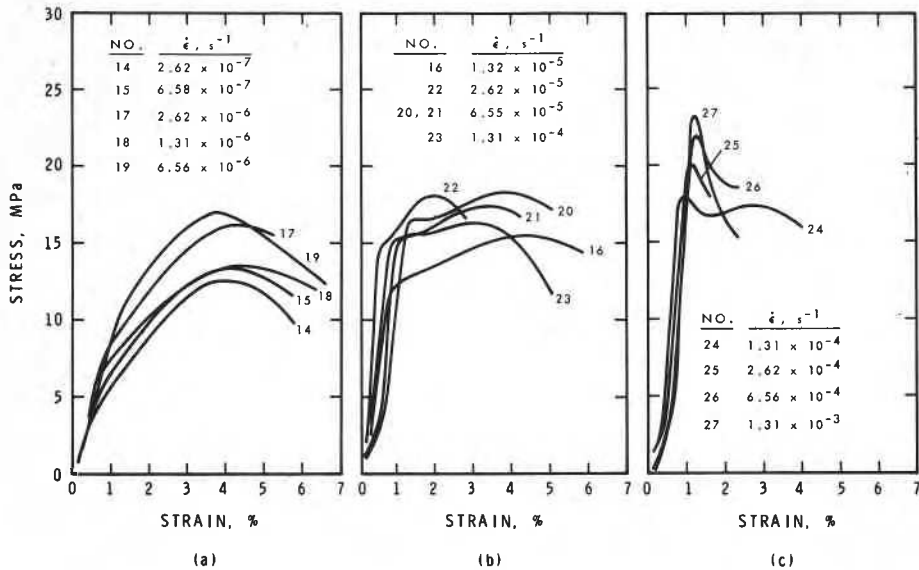
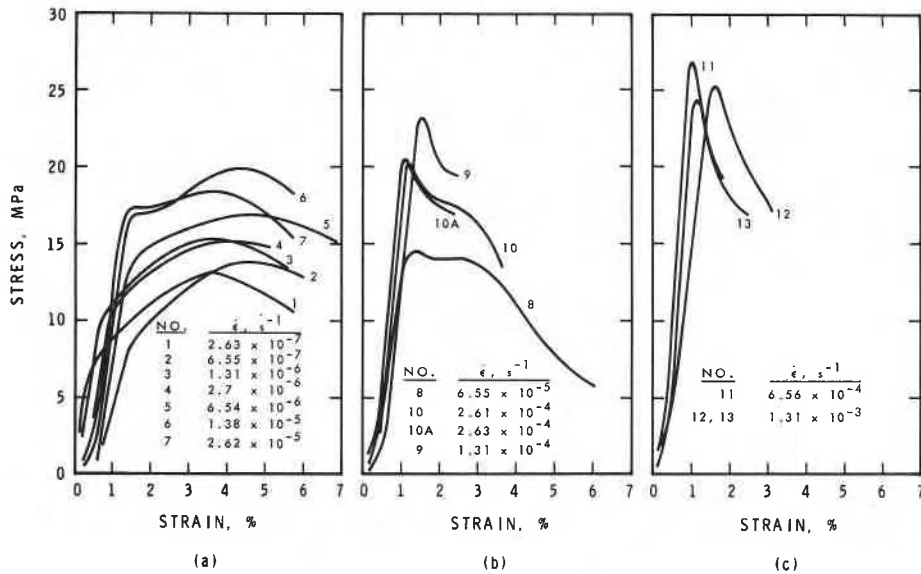
FIG. 3. Stress-strain curves for frozen sand at -2°C .FIG. 4. Stress-strain curves for frozen sand at -6°C .

testing machine of 25 000 kg (25 tons) capacity, inside a cold room maintained at $-6 \pm 0.2^{\circ}\text{C}$. Each test was carried out at a constant strain rate. To maintain constant specimen temperature during the test and to prevent sublimation of moisture from the surface, the sample was immersed in a kerosene bath. The bath temperature was maintained with an immersed heat exchange coil through which methanol at a constant temperature was circulated from a Tenney refrigerating chamber. Figure 2 is a schematic diagram of the test apparatus. Measurements were made at strain rates ($\dot{\epsilon}$) varying between 10^{-7} and

10^{-2} s^{-1} and at temperatures (T) of -2 , -6 , -10 , and -15°C .

Results

Figures 3-6 show the stress-strain curves obtained for various samples tested under different strain rates and temperatures. Details concerning strain rates, temperatures, maximum stress observed, etc. are given in Table 1. The stresses and strains were calculated from the load-displacement charts from the testing machine. The general observations are as follows.

FIG. 5. Stress-strain curves for frozen sand at -10°C .FIG. 6. Stress-strain curves for frozen sand at -15°C .

1. Specimens deform elastically in the early stages of deformation, i.e., for strains less than 1%. The transition from elastic to plastic deformation is not sharp at high temperatures (-2 and -6°C) and at low strain rates.

2. As the strain rate increases, the specimens show an upper yield point at the end of the elastic region and a small drop in stress before plastic deformation starts.

3. For tests at low strain rates, the specimens deform plastically to some extent (up to 4%) before attaining the maximum stress at which failure occurs. At higher strain rates, the maximum stress occurs soon after the end of the elastic region, with very little plastic deformation occurring (Figs. 3c; 4c; 5c; 6 b,c). In these cases the maximum stress (i.e., compressive strength) coincides with the upper yield stress. These specimens fail essentially in a brittle

TABLE 1. Values of the compressive failure strength (maximum stress observed), and initial tangent modulus for frozen sand, at various strain rates and temperatures

-15°C				-10°C				-6°C				-2°C			
Test No.	Strain rate, $\dot{\epsilon}$ (s ⁻¹)	σ_{max} (MPa)	E_i (MPa)	Test No.	Strain rate, $\dot{\epsilon}$ (s ⁻¹)	σ_{max} (MPa)	E_i (MPa)	Test No.	Strain rate, $\dot{\epsilon}$ (s ⁻¹)	σ_{max} (MPa)	E_i (MPa)	Test No.	Strain rate, $\dot{\epsilon}$ (s ⁻¹)	σ_{max} (MPa)	E_i (MPa)
(1)	(2)	(3)	(4)	(5)	(6)	(7)	(8)	(9)	(10)	(11)	(12)	(13)	(14)	(15)	(16)
1	2.63×10^{-7}	13.1		14	2.62×10^{-7}	12.55		41	1.65×10^{-7}	9.02		31	2.62×10^{-7}	6.81	
2	6.55×10^{-7}	13.83	962	15	6.58×10^{-7}	13.37		43	6.0×10^{-7}	10.30		34	6.55×10^{-7}	7.84	
3	1.31×10^{-6}	15.26	1644	16	1.32×10^{-6}	15.47	1945	44	2.38×10^{-6}	12.38	1389	33	6.55×10^{-6}	12.50	521
4	2.7×10^{-6}	15.21	1875	17	2.62×10^{-6}	16.14	1072	45	1.20×10^{-5}	12.96	2000	29	1.31×10^{-5}	10.79	595
5	6.54×10^{-6}	16.86	1607	18	1.31×10^{-6}	13.50		46	1.25×10^{-5}	12.52	2000	32	1.31×10^{-5}	12.77	595
6	1.38×10^{-5}	19.96	1833	19	6.56×10^{-6}	16.99		47	3.98×10^{-5}	13.70		30	2.62×10^{-5}	13.90	541
7	2.62×10^{-5}	17.37	2500	20	6.55×10^{-6}	18.29		48	1.25×10^{-4}	16.29	2333	28	6.55×10^{-5}	11.67	1000
8	6.55×10^{-5}	14.56		21	6.56×10^{-5}	17.37	2609	49	5.15×10^{-4}	14.82	3530	35	1.31×10^{-4}	13.81	1167
9	1.31×10^{-4}	23.13	2553	22	2.62×10^{-5}	18.08		50	5.53×10^{-4}	14.17	2619	36	2.62×10^{-4}	13.16	1216
10	2.61×10^{-4}	20.16	2500	23	1.31×10^{-4}	16.39	2273	51	1.31×10^{-3}	15.10	3333	37	6.55×10^{-4}	11.89	2500
10A	2.63×10^{-4}	20.51	2917	24	1.31×10^{-4}	18.00	3147	52	2.62×10^{-3}	17.00	3125	38	1.31×10^{-3}	13.09	2692
11	6.56×10^{-4}	26.84	3958	25	2.62×10^{-4}	20.04	2895	53	5.45×10^{-3}	19.53	3750	58	1.97×10^{-5}	12.81	
12	1.31×10^{-3}	25.26	2162	26	6.56×10^{-4}	21.88		54	1.19×10^{-2}	21.83	4822	59	1.98×10^{-6}	10.21	
13	1.31×10^{-3}	24.36	3600	27	1.31×10^{-3}	23.18	4167					60	3.95×10^{-7}	7.11	
												61	1.31×10^{-7}	5.14	
												62	3.95×10^{-6}	13.49	
												63	1.31×10^{-4}	12.27	
												64	3.91×10^{-4}	10.59	
												65	1.97×10^{-3}	13.48	

NOTE: 1 MPa = 10.2 kg/cm² = 145.06 psi.

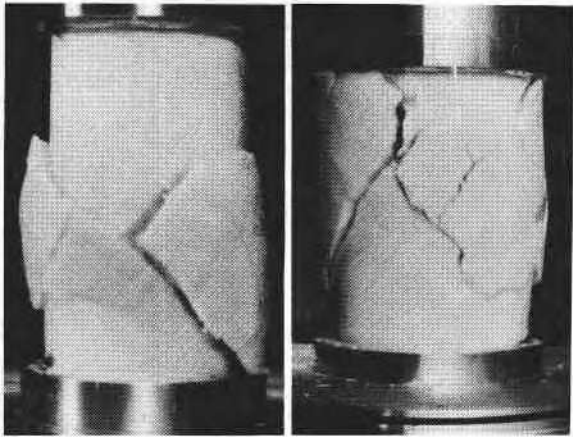


FIG. 7. Typical brittle fractures observed at high strain rates (temperature = -6°C , $\dot{\epsilon} > 10^{-3} \text{ s}^{-1}$).

manner. Figure 7 shows typical brittle fractures observed at high strain rates.

4. The maximum stress observed at the beginning of failure increased with increasing rates of strain and with decreasing temperature. For the range of strain rates investigated, namely 10^{-7} to 10^{-2} s^{-1} , the strength was found to increase linearly with strain rate on a log-log scale, for temperatures at and below -6°C (Fig. 8a). There was no change of slope for linear behaviour. At -2°C , a distinct transition was observed at a strain rate of about 10^{-5} s^{-1} . The variation of strength with strain rate at -2°C is shown in Fig. 8b. For strain rates smaller than 10^{-5} s^{-1} , the strength increased linearly with increasing strain rate. For strain rates larger than 10^{-5} s^{-1} , the strength appeared to be independent of strain rates. This can also be seen from the stress-strain curves shown in Fig. 3. The straight lines plotted in Fig. 8a for temperatures -6 , -10 , and -15°C , respectively, are least squares lines fitted by linear regression analysis of the data. Figure 9 shows the maximum failure stress (strength) plotted as a function of

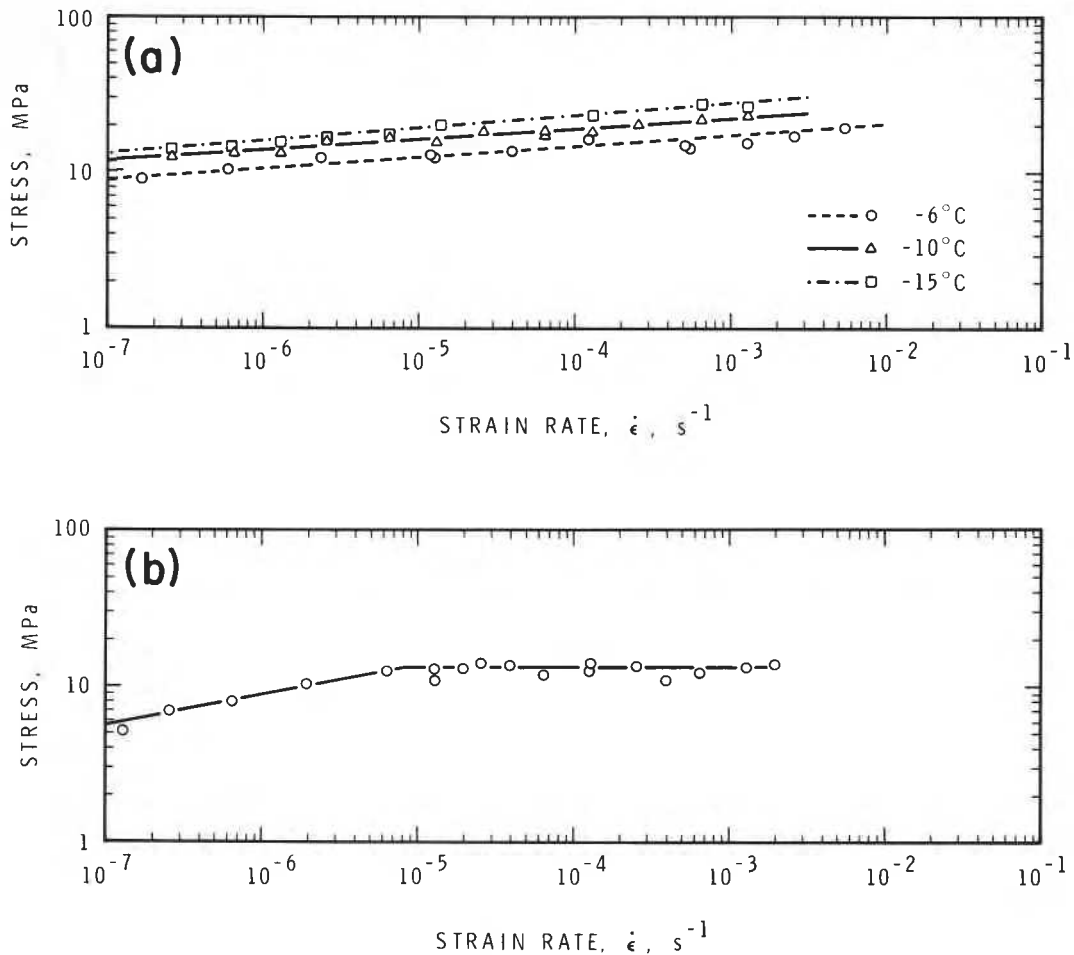


FIG. 8. Variation of compressive strength with strain rate: (a) at -6 , -10 , and -15°C ; and (b) at -2°C .

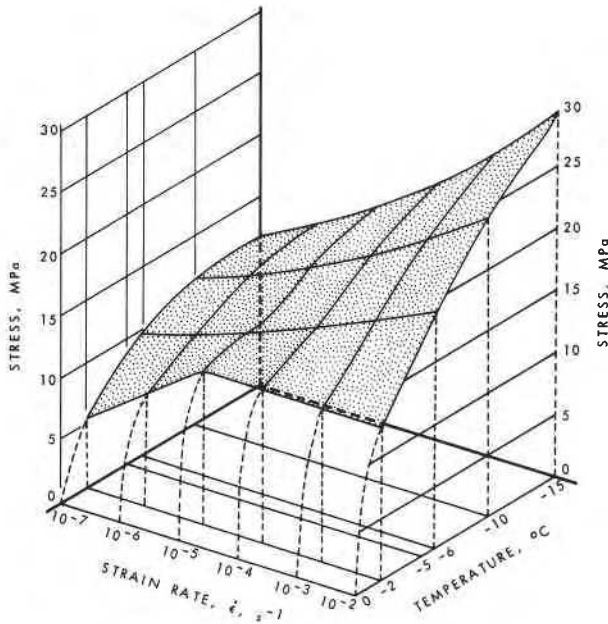


FIG. 9. Composite diagram showing compressive strength as a function of temperature and strain rate.

temperature and strain rate in a three-dimensional plot.

5. The slope of the initial elastic (or pseudoelastic) region of the stress-strain curve (called the initial

tangent modulus E_i) increased with increasing strain rates, at a particular temperature. Table 1 also gives values of the initial tangent modulus E_i from various tests. The variation of the initial tangent modulus with strain rate is shown in Fig. 10 *a* and *b*.

Discussion

Initial Yield and Plastic Flow

The initial yield stress observed in samples tested at low temperatures and high strain rates (for example, samples 16-23 in Fig. 5*b*; 5-7 in Fig. 6*a*), has been attributed to yielding of the ice matrix (Sayles 1974; Parameswaran and Jones 1980). After this initial yield, the stress drops because the stress required to maintain the strain rate is smaller than that required to initiate the yield. Such yield drops have been observed in many other materials such as carbon steels, ionic crystals, silicon, and germanium, although the mechanism involved is entirely different from that occurring in frozen sand. The increase in stress after the yield drop is due to the development of the frictional component of strength. This frictional component develops rapidly with slow rates of deformation under uniaxial compression and hence, at low strain rates, one does not observe the yield drop. At high strain rates, lack of confining pressure permits rupture of the sample prior to development of the full frictional component. This was confirmed

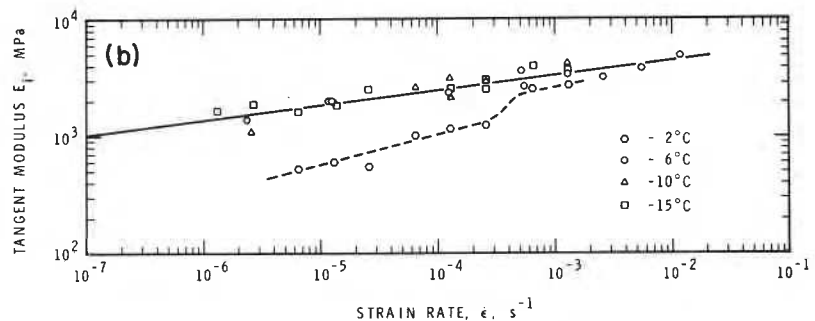
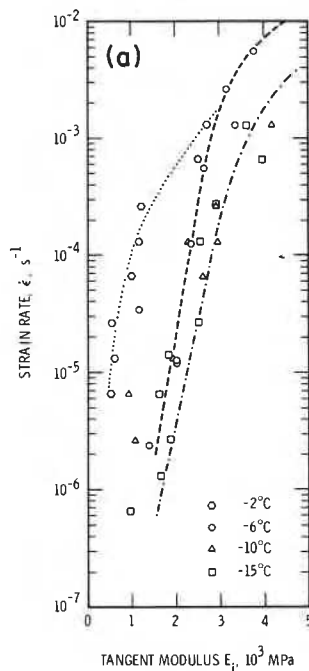


FIG. 10. Variation of initial tangent modulus: (a) with log (strain rate); and (b) with strain rate (log-log scale).

TABLE 2. Strength of frozen sand at various strain rates and temperatures obtained by different authors

Authors	Temperature (°C)	Strain rate (s ⁻¹)	Maximum stress (MPa)	Material and test method
Sayles (1966)	-40	5.5×10^{-4}	38.6	Saturated Ottawa fine sand (average grain dia. = 0.2-0.6 mm), constant rate compression tests
	-50 to -186	5.5×10^{-4}	35.9	(Stress independent of temp. below -50°C)
Sayles and Epanchin (1966)	-3	3.33×10^{-4} to 2.5×10^{-2}	10.35-15.86	Saturated Ottawa fine sand (average grain dia. = 0.2-0.6 mm), constant rate compression tests
	-6.5	3.33×10^{-4} to 2.5×10^{-2}	13.79-20.69	
	-10	3.33×10^{-4} to 2.5×10^{-2}	17.93-27.58	
	-30	3.33×10^{-4} to 2.5×10^{-2}	28.96-48.27	
Sayles (1968)	-10	5.5×10^{-4}	17.44	Saturated Ottawa fine sand (average grain dia. = 0.2-0.6 mm), constant rate compression tests
	-4.2	5.5×10^{-4}	10.10	
	-1.7	5.5×10^{-4}	9.10	
	-0.56	5.5×10^{-4}	5.14	
Sayles (1974)	-3.85	1.67×10^{-6} to 1.67×10^{-2}	8-17	Saturated Ottawa fine sand (average grain dia. = 0.2-0.6 mm), constant rate compression tests
Goughnour and Andersland (1968)	-3.85	4.43×10^{-6}	5.38	Saturated Ottawa fine sand (average grain dia. = 0.2-0.6 mm), constant rate compression tests
	-12.0	2.22×10^{-6}	8.27	
	-12.0	4.43×10^{-6}	9.38	
	-7.55	4.43×10^{-6}	7.59	
Alkire and Andersland (1973)	-12	4.43×10^{-6}	~7	Saturated silica sand (average particle dia. = 0.6-0.84 mm), constant rate compression tests
	-12	10^{-7} - 10^{-6}	0.5-6.0	
Chamberlain <i>et al.</i> (1972)	-10	9.67×10^{-4}	24.55	Saturated Ottawa banding sand, 0.1-0.2 mm dia., constant rate test under 3.5 MPa confining pressure
Ladanyi and Arteau (1978)	-5	1.67×10^{-8} to 1.67×10^{-3}	3-11	Saturated quartz sand from St. Canut, Quebec, 0.26-0.6 mm dia., constant rate compression tests
Eckardt (1978)	-15	2.1×10^{-7}	4.0	Frozen medium sand (water content = 12%), constant rate compression tests
		9.72×10^{-7}	6.0	
		4.07×10^{-6}	7.0	
		1.53×10^{-5}	8.0	
Parameswaran and Jones (1979)	-12	10^{-6} - 10^{-2}	16-28	Saturated Ottawa fine sand, constant rate tests under confining pressure of 5 MPa
Parameswaran (present results)	-2	10^{-7} - 10^{-2}	6-12.5	Saturated Ottawa fine sand, constant rate uniaxial compression tests
	-6	10^{-7} - 10^{-2}	10-20	
	-10	10^{-7} - 10^{-2}	11.5-25	
	-15	10^{-7} - 10^{-2}	12-29	

by Parameswaran and Jones (1980) who observed that in samples of the same material tested at a particular strain rate ($7.7 \times 10^{-5} \text{ s}^{-1}$) under triaxial conditions, increased hydrostatic confining pressure suppressed the yield drop and decreased the tendency of brittle fracture, thereby allowing the specimen to deform plastically prior to failure.

Comparison of the Present Results with Earlier Work

It is worthwhile to compare the present results with some earlier work on similar materials under conditions very similar to those used here. Table 2 gives the values of the maximum stress (or strength of the material) observed under various temperatures and strain rates by different authors. These data and the

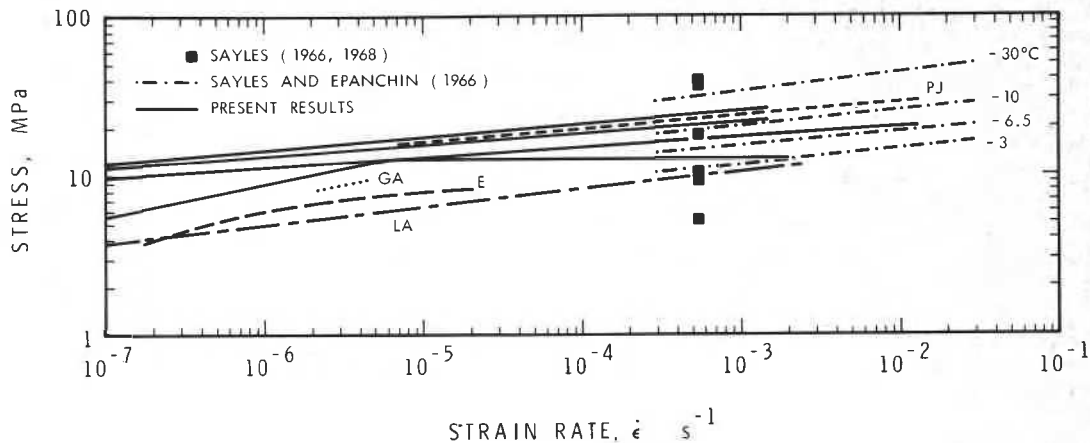


FIG. 11. Comparison of the results obtained in this study with those of other authors. PJ = Parameswaran and Jones (1979); GA = Goughnour and Andersland (1968); E = Eckardt (1978); LA = Ladanyi and Arteau (1978).

present results are plotted in Fig. 11, which shows that the present results fall closely in line with the data of Sayles (1966, 1968), and Sayles and Epanchin (1966). This is not fortuitous, because the material and sample preparation technique, and to some extent the testing methods, used in the present experiments were very similar to those used by Sayles (1968). The data of Parameswaran and Jones (1980), obtained under triaxial conditions at -12°C (line PJ in Fig. 11), lie between the present lines for -10 and -15°C and parallel to them. The data of Ladanyi and Arteau (1978) for -5°C fall consistently below the present line for -6°C ; however, they also find a linear increase of strength with increasing strain rates on a log-log scale, for a wide range of strain rates.

Strain-rate-dependence of Strength

The linear variation of strength with strain rate on a log-log scale in Fig. 8a indicates that these two quantities can be related to each other by an empirical power law equation of the type

$$[1] \quad \sigma_{\max} \propto (\dot{\epsilon})^m$$

or

$$[2] \quad \dot{\epsilon} \propto (\sigma_{\max})^n$$

where $n = 1/m$. The values of m and n obtained by linear regression analysis of the data at various temperatures are:

T ($^{\circ}\text{C}$)	m	n
-6	0.073	13.74
-10	0.071	14.14
-15	0.079	12.73

An empirical relationship similar to [2] has been observed earlier by Sayles and Epanchin (1966) and Sayles (1974) for Ottawa sand having the same density and moisture content as the present samples. For strain rates between 1.67×10^{-4} and $2 \times 10^{-2} \text{ s}^{-1}$, Sayles and Epanchin (1966) obtained the following values for the exponents m and n :

T ($^{\circ}\text{C}$)	m	n
-3	0.105	9.52
-6.5	0.092	10.87
-10	0.094	10.67

Values of 0.1 and 10 for m and n , respectively, for strain rates between 1.67×10^{-5} and $1.67 \times 10^{-2} \text{ s}^{-1}$, were obtained by Sayles (1974) from triaxial constant strain-rate tests at -3.85°C .

In the present series of tests at -2°C (Fig. 8b), a transition in the mode of deformation behaviour is indicated for strain rates below $6 \times 10^{-6} \text{ s}^{-1}$. Earlier authors (Sayles and Epanchin 1966; Sayles 1974) did not see this transition in frozen sand, probably because they did not test at low enough strain rates (lower than 10^{-4} s^{-1}).

Such a transition in the mode of failure, indicated by a change in slope for the $\log(\sigma)$ versus $\log(\dot{\epsilon})$ curve, has been observed in ice. Dillon and Andersland (1967) analyzed the experimental creep data available in the literature and found that a transition from one mode of creep behaviour to another occurs for ice at a strain rate of about $1.67 \times 10^{-7} \text{ s}^{-1}$, for temperatures as low as -15°C . They postulated that the behaviour in the low strain-rate region could be explained by creep occurring at the grain boundaries

in ice, with diffusion or accommodation cracking taking place primarily at grain boundaries. Barnes *et al.* (1971) have suggested that for moderate stresses at temperatures between -8 and -1°C , creep in polycrystalline ice is associated with both a liquid phase at the grain boundaries and grain boundary sliding. Combining these postulates with the present experimental observation at -2°C , it is presumed that the low strain-rate behaviour is governed by the unfrozen water content in the frozen sand specimens. For sand, the unfrozen water content is 0.2% by weight at -0.5°C , but 0 at -4°C and below (Tsytoich 1975). At -2°C , there is still some unfrozen water (although negligible) around each sand grain.

Anderson *et al.* (1973) proposed an equation to calculate the unfrozen water content, W_u , at any temperature below freezing, using the specific surface area, S , of the soil grains.

$$[3] \ln(W_u) = a + b \ln(S) + C(S)^d \ln(\theta)$$

When S is expressed in square metres per gram and θ is the soil temperature in degrees Celsius below freezing, W_u is obtained as gram H_2O per gram soil. Values of the constants a , b , c , and d , determined from isothermal calorimetric measurements of specific heat capacities of various representative soils, were: $a = 0.2618$, $b = 0.5519$, $c = -1.449$, and $d = -0.2640$.

The specific surface area of Ottawa sand, calculated from grain-size analysis, was $0.0056 \text{ m}^2/\text{g}$. Using this value of S and the values of a , b , c , and d in [3], the amount of unfrozen water content in Ottawa sand at -2°C (i.e., $\theta = 2$) is $0.001433 \text{ g H}_2\text{O}$ per gram soil or 0.1433% by weight. This is a negligible quantity for practical purposes and is too small to be measured by any physical methods.

The amount of unfrozen water around each grain, however, is increased considerably due to pressure melting of ice, caused by stress at the interparticle contact point. For example, the pressure at the contact point of a rounded quartz grain of 1 mm (0.04 in.) diameter with a flat ice interlayer (elastic moduli for quartz and ice being $2.94 \times 10^4 \text{ MPa}$ ($4.26 \times 10^6 \text{ psi}$) and $2.94 \times 10^3 \text{ MPa}$ ($4.26 \times 10^5 \text{ psi}$) respectively), calculated by Tsytoich (1975) from Hertz formulae in elasticity theory, was about 115 MPa under an external pressure of 0.2 MPa . This shows that the external applied force is multiplied by a factor of about 575 or more, at the interparticle contact point. For two hard particles the factor is even larger. Using this factor, an external load of 5 MPa (725 psi) will become 2875 MPa ($4.17 \times 10^5 \text{ psi}$) at the interparticle contact points. This

pressure is almost equal to the value of the theoretical elastic shear modulus for ice, and high enough to cause pressure melting at the interparticle junction. At a temperature of -2°C all the water may not be able to freeze during the test, and at low enough strain rates, it could migrate within the soil sample and cause a low value of strength. Hence there is the drop in the curve for -2°C below a strain rate of 10^{-6} s^{-1} .

From the slope of the straight line portion of the curve in Fig. 8b, where the strength depends on strain rate, the calculated value of the exponent n was 5.41. This is very close to the value of $n = 5$ observed by Ramseier (1972) in polycrystalline natural ice under steady-state creep conditions, when stresses are high enough to induce cracking and failure.

Temperature-dependence of Strength

Several authors have attempted to apply the theory of rate processes proposed by Glasstone *et al.* (1941) to explain the temperature-dependence of strength of frozen and unfrozen soils (Alkire and Andersland 1973; Andersland and Akili 1967; Andersland and AlNouri 1970; Goughnour and Andersland 1968; Hooke *et al.* 1972; Mitchell *et al.* 1968; Vyalov 1965a,b, 1978a,b). The theory of absolute reaction rates, commonly known as the rate process theory, can be applied to any process involving the time- and temperature-dependent rearrangement of matter, and hence it was thought that this theory could appropriately describe and predict soil behaviour under stresses. According to the theory, the deformation of frozen soil can be considered as a thermally activated process. General expressions relating the rate of deformation $\dot{\epsilon}$, temperature T , and stress σ are as follows:

$$[4] \dot{\epsilon} = \dot{\epsilon}_0 \exp(-\Delta G/RT) \exp B\sigma$$

$$[5] \dot{\epsilon} = C\sigma^n \exp(-\Delta G/RT)$$

In these equations, $\dot{\epsilon}_0$ and C are frequency factors that depend on the thermal fluctuations or frequency of thermal activation; ΔG is an activation energy to be supplied for each activation process; and B is a factor having dimensions of $(\text{stress})^{-1}$. The parameters $\dot{\epsilon}_0$, C , and ΔG are functions of temperature, stress, and the structure of the material at the instant of measurement. Assuming that the soil structure, the parameters $\dot{\epsilon}_0$ and B , and the activation energy ΔG are relatively insensitive to small changes in temperature, one can differentiate [4] after taking logarithms of both sides and obtain:

$$[6] R \partial \ln(\dot{\epsilon}/\dot{\epsilon}_0)/(\partial(1/T)) = -\Delta G$$

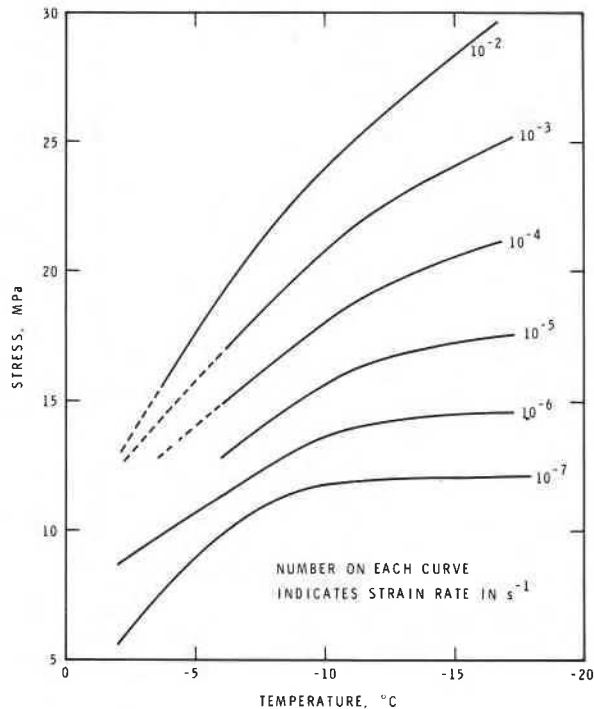


FIG. 12. Variation of compressive strength as a function of temperature. (Number on each curve indicates strain rate in s^{-1} .)

Thus, from a plot of $\ln(\dot{\epsilon})$ versus $1/T$ for constant stress, the activation energy, ΔG , can be calculated from the slope of the straight line. For a single thermally activated process, the activation energy should be constant at a particular stress.

In order to apply the theory of the thermally activated deformation process to the present results, the data shown in Fig. 8 *a* and *b* were replotted as shown in Fig. 12, where strength is plotted against temperature for various strain rates. Table 3 shows the values of strain rate and temperature for each stress value, obtained from Fig. 12. Figure 13 shows the logarithm of strain rates plotted against $1/T$ for each stress. The slopes of the lines change continuously, and no unique activation energy can be calculated from Fig. 13, perhaps because more than one deformation mechanism, each having a different activation energy, may be involved.

Glen (1975) has pointed out that the theory of thermally activated plastic flow governed by an Arrhenius equation of type [4] can be applied to ice only at temperatures below -10°C . Above this temperature, the Arrhenius equation breaks down and, as pointed out earlier, other processes such as grain boundary flow and liquid phase transport (to

TABLE 3. Values of strain rates ($\dot{\epsilon}$), and temperatures (T) corresponding to different strength values (from Fig. 10)

σ (MPa) (1)	$\dot{\epsilon}$ (s^{-1}) (2)	T ($^{\circ}\text{C}$) (3)	T ($^{\circ}\text{K}$) (4)	$\frac{1}{T} \times 10^4$ ($^{\circ}\text{K}^{-1}$) (5)
9	10^{-6}	-2.4	270.6	36.95
	10^{-7}	-5	268	37.31
10	10^{-6}	-4.95	268.05	37.31
	10^{-7}	-6.2	266.8	37.48
11	10^{-6}	-5.5	267.5	37.38
	10^{-7}	-7.8	265.2	37.71
12	10^{-6}	-4.8	268.2	37.29
	10^{-6}	-7.1	265.9	37.61
	10^{-7}	-13.5	259.5	38.54
13	10^{-5}	-6.2	266.8	37.48
	10^{-6}	-8.8	264.2	37.85
14	10^{-2}	-2.7	270.3	37.00
	10^{-3}	-3.4	269.6	37.09
	10^{-4}	-5	268	37.31
	10^{-5}	-7.6	265.4	37.68
	10^{-6}	-11.4	261.6	38.23
	10^{-7}	-13.5	259.5	38.54
15	10^{-2}	-3.35	269.65	37.09
	10^{-3}	-4.3	268.7	37.22
	10^{-4}	-6.2	266.8	37.48
	10^{-5}	-9	264	37.88
	10^{-6}	-13.5	259.5	38.54
16	10^{-2}	-4	269	37.17
	10^{-3}	-5.2	267.8	37.34
	10^{-4}	-7.5	265.5	37.66
	10^{-5}	-10.7	262.3	38.12
17	10^{-2}	-4.6	268.4	37.26
	10^{-3}	-6.2	266.8	37.48
	10^{-4}	-8.7	264.3	37.84
	10^{-5}	-14	259	38.61
18	10^{-2}	-5.3	267.7	37.36
	10^{-3}	-7.15	265.85	37.62
	10^{-4}	-10	263	38.02
19	10^{-2}	-6	267	37.45
	10^{-3}	-8.1	264.9	37.75
	10^{-4}	-11.5	261.5	38.24
20	10^{-2}	-6.7	266.3	37.55
	10^{-3}	-9.2	263.8	37.91
	10^{-4}	-13.7	259.3	38.57
21	10^{-2}	-7.4	265.6	37.65
	10^{-3}	-10.25	262.75	38.06
	10^{-4}	-16.5	256.5	38.99
23	10^{-2}	-9.1	263.9	37.89
	10^{-3}	-13.1	259.9	38.48
25	10^{-2}	-11.1	261.9	38.18
	10^{-3}	-17	256	39.06

be discussed in a subsequent section) govern the deformation behaviour. In the case of frozen sand, this transition temperature could be further lowered since the stresses at the interparticle junctions cause pressure melting of the ice matrix.

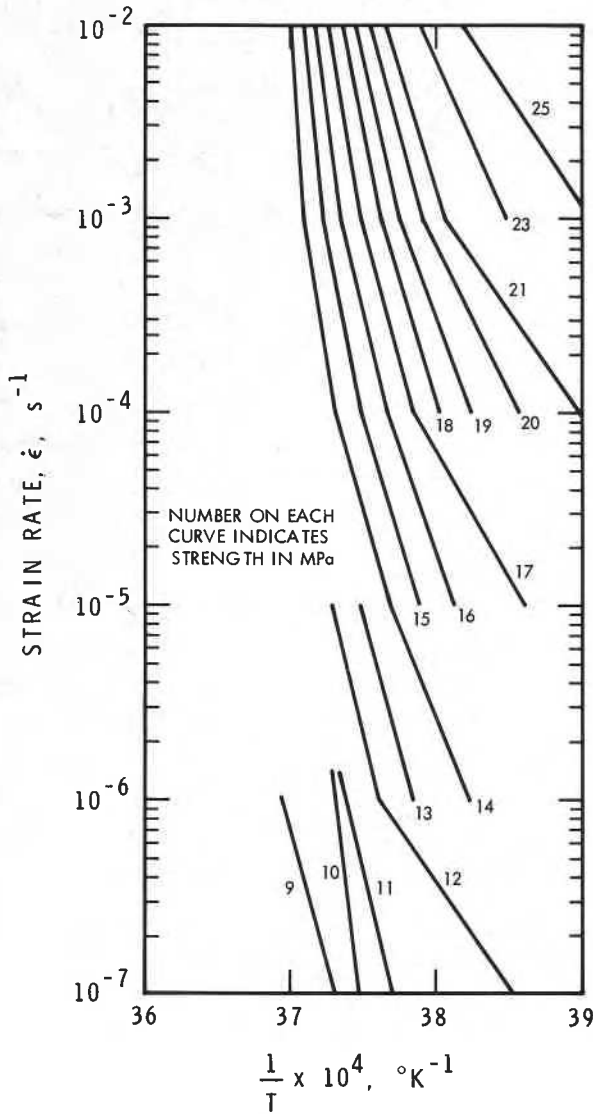


FIG. 13. Variation of log (strain rate) with $1/T$ for various stresses, from Table 3. (Number on each curve indicates stress in MPa.)

Figure 14 shows the strength values plotted against temperature, θ (degrees Celsius below freezing), on a log-log scale, for various strain rates. At higher strain rates, linear variation is seen and the slope of the lines is about 0.44. This suggests that strength varies with temperature according to an equation

$$[7] \quad \sigma \propto \theta^s$$

where $s = 0.44$.

A similar equation was proposed earlier by Tsytovich (1975) and a value of $s = 0.5$ was observed in some of his experiments. Figure 15 shows the strain

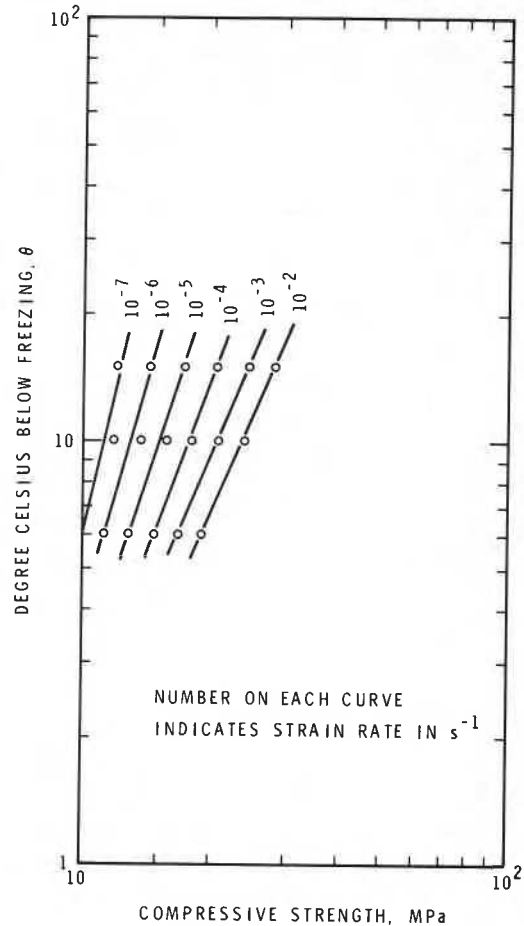


FIG. 14. Variation of compressive strength with degrees Celsius below freezing. (Number on each curve indicates strain rate in s^{-1} .)

rates plotted against temperature, θ (degrees Celsius below freezing), for various values of peak stress. Here again a linear variation was observed with almost the same slope for the higher strain-rate region ($> 10^{-5} s^{-1}$).

The present data show that the temperature dependence of strength cannot be explained by a thermally activated theory of deformation, but by the simple power law proposed by Tsytovich (1975). Further experiments at lower temperatures are in progress to see if the deformation process at lower temperatures can be associated with a thermally activated process.

Deformation of frozen sand occurs mainly by deformation occurring in the ice phase with mobilization of soil grain friction at the later stages of deformation. An appropriate model that could be used to depict this behaviour is that of the flow of a

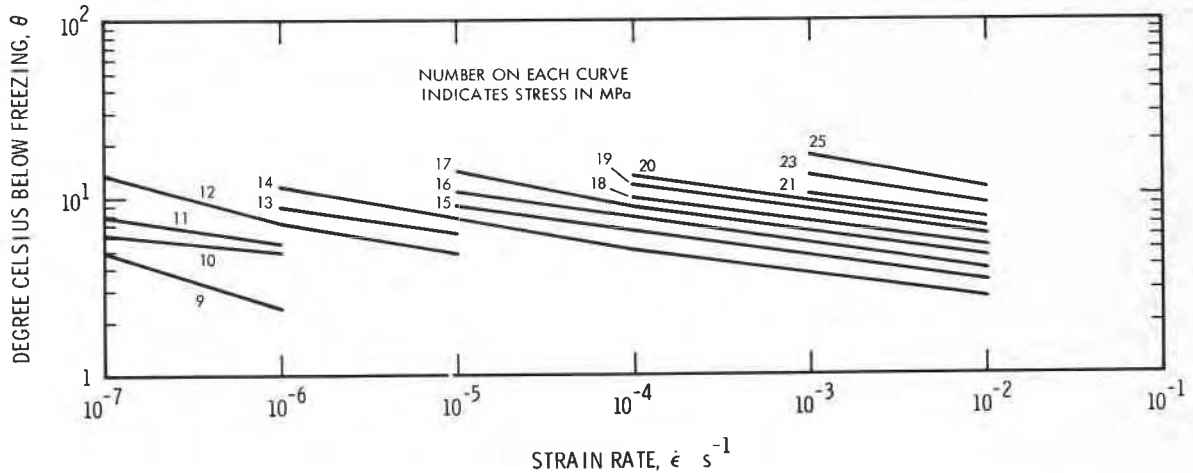


FIG. 15. Variation of strain rate with degrees Celsius below freezing, for constant stress values, from Table 3. (Number on each curve indicates stress in MPa.)

material in presence of an aqueous fluid phase or partial melt, which is a model of fluid phase transport. The model is based on the idea that a deviatoric stress causes difference in pressure between points of contact of granules, which in turn leads to a chemical potential of ions between those points where the pressure is high and those where it is lower. The parallel to this is Coble creep at high temperature in polycrystalline single-phase materials where the diffusive transport occurs through the grain boundary (Coble 1963). In frozen sand, the fluid phase simply replaces the grain boundary as a diffusive path. In such a material where liquid transport brings about deformation, a change in temperature can alter the proportion of the liquid phase and a spurious effect due to structural change is also introduced. Hence the usual temperature-change experiments may not give appropriate activation energies.

The model is essentially a qualitative one. Gittus (1977, 1978) has applied the model somewhat quantitatively to deformation of superplastic alloys at elevated temperatures.

Strain-rate- and Temperature-dependence of the Initial Tangent Modulus

Although the behaviour of soil may not be strictly represented as linear elastic, solutions based on the assumption of linear elastic behaviour are commonly used for estimation of stresses in the field. For this, a knowledge of the initial tangent modulus E_i is needed. Knowledge of E_i is also essential to predict the dynamic response of frozen ground when geophysical exploration techniques are used or when the region is hit by an earthquake.

Values of the initial tangent modulus calculated from the slopes of the early elastic (or pseudoelastic) part of the stress-strain curves (Figs. 3-6) are shown in Table 1. The modulus E_i was found to increase with increasing strain rates and decreasing temperature. Figure 10a shows the initial tangent modulus plotted against log (strain rates) for various temperatures. Figure 10b shows the modulus plotted against strain rates on a log-log scale. In this figure it can be seen that the modulus values at -2°C are considerably smaller than the values for lower temperatures, for the lower strain-rate region. At higher strain rates, the modulus tends to approach values closer to the low temperature values. The lower values of modulus at -2°C at the lower strain rates of deformation support the earlier proposition that the amount of unfrozen water at -2°C , under superimposed stresses, could be much larger than theoretically calculated from [3]; at lower strain rates, this water has sufficient time to migrate within the sample and reduce strength as well as modulus.

Conclusions

Uniaxial unconfined compression tests of cylindrical samples of frozen Ottawa sand containing about 20% by weight of water showed the following results.

1. Strength increases with increasing strain rates and decreasing temperatures. Between 10^{-7} and 10^{-2} s^{-1} , the strength showed a linear variation with strain rate on a log-log scale, for temperatures -6 , -10 , and -15°C . At -2°C , for strain rates lower than $6 \times 10^{-6} \text{ s}^{-1}$, the same linear increase of strength was observed with a steeper slope, but for

strain rates larger than 10^{-5} s^{-1} , the strength was not dependent on the strain rate.

2. The initial tangent modulus, E_i , increased with increasing strain rates. The variation was linear for temperatures -6 , -10 , and -15°C , on a log-log scale. At -2°C , the values of E_i were considerably smaller than those at lower temperatures. For strain rates larger than 10^{-5} s^{-1} , the values of E_i at -2°C tended to approach the values at lower temperatures.

3. The considerably lower values of modulus and strength at -2°C , as compared with those at lower temperatures, were probably due to larger amounts of unfrozen water present at -2°C . This unfrozen water exists due to the magnification of the superimposed stresses by a large factor at interparticle junctions, thereby causing pressure melting to occur.

4. Analysis of the present data according to the theory of thermally activated deformation process could not give a unique activation energy. Instead, the data could be fitted reasonably well to simple power laws relating strength and strain rate, and strain rate and temperature.

Acknowledgements

The author acknowledges with pleasure the assistance of G. Mould and C. Hubbs in the laboratory. The author expresses his sincere thanks to his colleague, Harry Baker, for some useful discussions on the testing of frozen sands. Thanks are also due to Dr. Stephen Jones of the Glaciology Division, Department of Fisheries and Environment, for the use of the low temperature Tenney refrigeration unit.

This paper is a contribution from the Division of Building Research, National Research Council of Canada, and is published with the approval of the Director of the Division.

- ALKIRE, B. D., and ANDERSLAND, O. B. 1973. The effect of confining pressure on the mechanical properties of sand ice materials. *Journal of Glaciology*, **12**, pp. 469-481.
- ANDERSLAND, O. B., and AKILI, W. 1967. Stress effect on creep rates of a frozen clay soil. *Géotechnique*, **17**, pp. 27-39.
- ANDERSLAND, O. B., and ALNOURI, I. 1970. Time-dependent strength behaviour of frozen soil. *ASCE Journal of the Soil Mechanics and Foundations Division*, **96(SM4)**, pp. 1249-1265.
- ANDERSON, D. M., TICE, A. R., and MCKIM, H. L. 1973. The unfrozen water and the apparent specific heat capacity of frozen soils. *Permafrost, North American Contribution to the 2nd International Conference*, National Academy of Sciences, Washington, DC, pp. 289-295.
- BAKER, T. H. W. 1976. Preparation of artificially frozen sand specimens. Division of Building Research, National Research Council of Canada, Ottawa, Ont., NRCC 15349.
- BARNES, P., TABOR, D., and WALKER, J. C. 1971. The friction and creep of polycrystalline ice. *Proceedings, Royal Society of London*, **A.324**, pp. 127-155.
- CHAMBERLAIN, E., GROVES, C., and PERHAM, R. 1972. The mechanical behaviour of frozen earth materials under high pressure triaxial test conditions. *Géotechnique*, **22**, pp. 469-483.
- COBLE, R. L. 1963. A model for boundary diffusion controlled creep in polycrystalline materials. *Journal of Applied Physics*, **34**, pp. 1679-1682.
- DILLON, H. B., and ANDERSLAND, O. B. 1967. Deformation rates of polycrystalline ice. *Physics of Snow and Ice, Proceedings, International Conference on Low Temperature Science*, The Institute of Low Temperature Science, Hokkaido University, Sapporo, Japan, pp. 313-328.
- ECKARDT, H. 1978. Creep behaviour of frozen soils in uniaxial compression tests. *Proceedings, International Symposium on Ground Freezing*, Ruhr University, Bochum, Germany, Vol. 2, pp. 81-93.
- GITTUS, J. H. 1977. Theory of superplastic flow in two-phase materials: roles of interphase-boundary dislocations, ledges, and diffusion. *ASME Journal of Engineering Materials and Technology*, **99**, Series H, pp. 244-251.
- 1978. High-temperature deformation of two phase structures. *Philosophical Transactions, Royal Society of London*, **A.288**, pp. 121-146.
- GLASSTONE, S., LAIDLER, D., and EYRING, H. 1941. *The theory of rate processes*. McGraw-Hill Book Company, New York, NY.
- GLEN, J. W. 1975. The mechanics of ice. U.S. Army, Corps of Engineers, Cold Regions Science and Engineering Monograph II-C2b. 47 p.
- GOUGHNOUR, R. R., and ANDERSLAND, O. B. 1968. Mechanical properties of a sand-ice system. *ASCE Journal of the Soil Mechanics and Foundations Division*, **94(SM4)**, pp. 923-950.
- HOOKE, R. LEB., DAHLIN, B. B., and KAUPER, M. T. 1972. Creep of ice containing dispersed fine sand. *Journal of Glaciology*, **11**, pp. 327-336.
- LADANYI, B., and ARTEAU, J. 1978. Effect of specimen shape on creep response of a frozen sand. *Proceedings, International Symposium on Ground Freezing*, Ruhr University, Bochum, Germany, Vol. 1, pp. 141-153.
- MITCHELL, J. K., CAMPANELLA, R. G., and SINGH, A. 1968. Soil creep as a rate process. *ASCE Journal of the Soil Mechanics and Foundations Division*, **94(SM1)**, pp. 231-253.
- PARAMESWARAN, V. R. 1978a. Laboratory studies of the adfreeze bond between small scale model piles and frozen sand. *Proceedings, 3rd International Conference on Permafrost*, National Research Council of Canada, Ottawa, Ont., Vol. 1, pp. 714-720.
- 1978b. Adfreeze strength of frozen sand to model piles. *Canadian Geotechnical Journal*, **15**, pp. 494-500.
- 1979. Creep of model piles in frozen soil. *Canadian Geotechnical Journal*, **16**, pp. 69-77.
- PARAMESWARAN, V. R., and JONES, S. J. 1980. Triaxial testing of frozen sand. *Journal of Glaciology*. In press.
- RAMSEIER, R. O. 1972. Growth and mechanical properties of river and lake ice. Ph.D. thesis, Laval University, Quebec, P.Q.
- SAYLES, F. H. 1966. Low temperature soil mechanics—interim report. U.S. Army, Corps of Engineers, Cold Regions Research and Engineering Laboratory, Hanover, NH, Technical Note.
- 1968. Creep of frozen sands. U.S. Army, Corps of Engineers, Cold Regions Research and Engineering Laboratory, Hanover, NH, Technical Report No. 190.

- 1974. Triaxial constant strain rate tests and triaxial creep tests on frozen Ottawa sand. U.S. Army, Corps of Engineers, Cold Regions Research and Engineering Laboratory, Hanover, NH, Technical Report No. 253.
- SAYLES, F. H., and EPANCHIN, N. V. 1966. Rate of strain compression tests on frozen Ottawa sand and ice. U.S. Army, Corps of Engineers, Cold Regions Research and Engineering Laboratory, Hanover, NH, Technical Note.
- TSYTOVICH, N. A. 1975. The mechanics of frozen ground, McGraw-Hill Book Company, New York, NY.
- TSYTOVICH, N. A., and SUMGIN, M. I. 1959. Principles of mechanics of frozen ground. U.S. Army, Corps of Engineers, Cold Regions Research and Engineering Laboratory, Hanover, NH, Translation 19.
- TSYTOVICH, N. A., *et al.* 1973. Physics, physical chemistry and mechanics of permafrost and ice. U.S. Army, Corps of Engineers, Cold Regions Research and Engineering Laboratory, Hanover, NH, Draft Translation 439.
- VYALOV, S. S., *editor*. 1965a. The strength and creep of frozen soils and calculation for ice-soil retaining structures. U.S. Army, Corps of Engineers, Cold Regions Research and Engineering Laboratory, Hanover, NH, Translation 76.
- 1965b. Rheological properties and bearing capacity of frozen soils. U.S. Army, Corps of Engineers, Cold Regions Research and Engineering Laboratory, Hanover, NH, Translation 74.
- VYALOV, S. S. 1978a. Long-term rupture of permafrost as a thermally activated process. Permafrost, USSR Contribution to the 2nd International Conference, National Academy of Sciences, Washington, DC, pp. 223-228.
- 1978b. Kinetic theory of the deformation of frozen soils. Proceedings, 3rd International Conference on Permafrost, National Research Council of Canada, Ottawa, Ont., Vol. 1, pp. 750-755.
- VYALOV, S. S., and PORKHAEV, G. V. 1976. Handbook for the design of bases and foundations of buildings and other structures on permafrost. Translated by V. Poppe. National Research Council of Canada, Ottawa, Ont., Technical Translation No. 1865.